Coherent optical creation of a single molecule – Supplemental material

Yichao Yu,[1,2,3,*] Kenneth Wang,[1,2,3,†] Jonathan D. Hood,[4] Lewis R. B. Picard,[1,2,3]
Jessie T. Zhang,[1,2,3] William B. Cairncross,[2,1,3] Jeremy M. Hutson,[5]
Rosario Gonzalez-Ferez,[6,7] Till Rosenband,[8] and Kang-Kuen Ni[2,1,3,‡]

[1] *Department of Physics, Harvard University, Cambridge, Massachusetts 02138, USA*
[2] *Department of Chemistry and Chemical Biology, Harvard University, Cambridge, Massachusetts 02138, USA*
[3] *Harvard-MIT Center for Ultracold Atoms, Cambridge, Massachusetts 02138, USA*
[4] *Department of Chemistry, Purdue University, West Lafayette, Indiana, 47906, USA*
[5] *Joint Quantum Centre Durham-Newcastle, Department of Chemistry, Durham University, Durham, DH1 3LE, United Kingdom*
[6] *Instituto Carlos I de Física Teórica y Computacional, and Departamento de Física Atómica, Molecular y Nuclear, Universidad de Granada, 18071 Granada, Spain*
[7] *ITAMP, Harvard-Smithsonian Center for Astrophysics, Cambridge, Massachusetts 02138, USA*
[8] *Agendile LLC, Cambridge, Massachusetts 02139, USA*

(Dated: May 10, 2021)

S1. 3 LEVEL RAMAN TRANSFER WITH CROSS COUPLING

In our system, the separation in energy between the initial and target state is much smaller than the single photon detuning Δ from the intermediate state; see Fig. 1a in the main text. Thus, there is significant cross coupling for the scattering rate and light shift, where each state is coupled to the excited state by the power in both beams. Under these conditions, the scattering rate and light shift are proportional to the total power $P_{\mathrm{tot}} = P_{\mathrm{m}} + P_{\mathrm{a}}$, where $P_{\mathrm{m}}(P_{\mathrm{a}})$ is the power in the beam that addresses the molecular (atomic) state. The Raman Rabi frequency is proportional to $\sqrt{P_{\mathrm{m}} P_{\mathrm{a}}}$. With a fixed total power and thus fixed scattering rate, the Raman Rabi frequency is maximized when $P_{\mathrm{m}} = P_{\mathrm{a}} = P_{\mathrm{tot}}/2$.

For the purposes of this work, we denote $\Omega_{\mathrm{a}}(\Omega_{\mathrm{m}})$ as the Rabi frequencies to drive a transition from the atom (target molecule) state to the intermediate state used in the Raman transition corresponding to the power in a single beam, P_{a} (P_{m}). Thus, the Raman Rabi frequency is $\Omega_{\mathrm{a}}\Omega_{\mathrm{m}}/(2\Delta)$, where Δ is the single photon detuning. Cross coupling affects the scattering rate and light shift, and assuming equal powers in both beams, these quantities become $\Gamma_{\mathrm{e}}\Omega_{\mathrm{m}}^2/(2\Delta^2) + \Gamma_{\mathrm{e}}\Omega_{\mathrm{a}}^2/(2\Delta^2)$ and $\Omega_{\mathrm{m}}^2/(2\Delta) - \Omega_{\mathrm{a}}^2/(2\Delta)$, where Γ_{e} is the excited state linewidth. Since $\Omega_{\mathrm{m}} >> \Omega_{\mathrm{a}}$, the scattering rate and light shift can be approximated as $\Gamma_{\mathrm{e}}\Omega_{\mathrm{m}}^2/(2\Delta^2)$ and $\Omega_{\mathrm{m}}^2/(2\Delta)$.

S2. RAMAN TRANSFER WITH MANY INTERMEDIATE STATES

With multiple intermediate states, the total Raman Rabi frequency, scattering rate, and light shift become a sum over all these possible states. In our model, we consider all vibrational states of $c^3\Sigma^+(\Omega = 1)$ and states in the atomic continuum as intermediate states. The Rabi frequency between two states is proportional to the electronic dipole moment, arising from the electronic wavefunctions, and the overlap of the vibrational wavefunctions. Under the assumption that the electronic dipole moment d is the same for all transitions between the ground state and the excited electronic state, the total Raman Rabi frequency becomes

$$\Omega_{\mathrm{R}} = \frac{d^2 E^2}{2\hbar^2} \sum_{v'} \frac{\langle a|v'\rangle \langle v'|m\rangle}{\Delta_{v'}}, \tag{S.1}$$

where $|a\rangle$ ($|m\rangle$) are the relative coordinate wavefunctions for the trapped atomic (target molecular) state, and $|v'\rangle$ is the relative-coordinate wavefunction for the excited state which includes both bound molecular states and the atomic continuum. $\Delta_{v'}$ is a single photon detuning with respect to the $|v'\rangle$ state, E is the electric field for the power in the

* Y.Y. and K.W. contributed equally to this work.; yichaoyu@g.harvard.edu
† Y.Y. and K.W. contributed equally to this work.
‡ ni@chemistry.harvard.edu

single beam given a waist size. We can divide this sum into a sum over all the bound molecular states, and a sum over atomic continuum states,

$$\Omega_{\mathrm{R}} = \frac{d^2E^2}{2\hbar^2} \sum_{v' \leq v'_{\mathrm{max}}} \frac{\langle a|v'\rangle \langle v'|m\rangle}{\Delta_{v'}} + \frac{d^2E^2}{2\hbar^2} \sum_{v' > v'_{\mathrm{max}}} \frac{\langle a|v'\rangle \langle v'|m\rangle}{\Delta_{v'}}, \tag{S.2}$$

where v'_{max} corresponds to the excited molecular state, which is most weakly bound. The first term can be calculated numerically given an excited state potential. To calculate the second term, we first make an assumption that we are far enough detuned from the contributing continuum states that they are all at approximately the same detuning, Δ_{thresh}. This allows us to pull it out of the sum, and we obtain

$$\Omega_{\mathrm{R}} \approx \frac{d^2E^2}{2\hbar^2} \sum_{v' \leq v'_{\mathrm{max}}} \frac{\langle a|v'\rangle \langle v'|m\rangle}{\Delta_{v'}} + \frac{d^2E^2}{2\hbar^2\Delta_{\mathrm{thresh}}} \sum_{v' > v'_{\mathrm{max}}} \langle a|v'\rangle \langle v'|m\rangle . \tag{S.3}$$

From requiring completeness and orthogonality,

$$\sum_{v'} \langle a|v'\rangle \langle v'|m\rangle = \langle a|m\rangle = 0, \tag{S.4}$$

we derive an expression for the second sum in equation S.3

$$\sum_{v' > v'_{\mathrm{max}}} \langle a|v'\rangle \langle v'|m\rangle = - \sum_{v' \leq v'_{\mathrm{max}}} \langle a|v'\rangle \langle v'|m\rangle , \tag{S.5}$$

which can be calculated from the vibrational states of the excited state potential. Thus, the Raman Rabi frequency can be approximated as:

$$\Omega_{\mathrm{R}} \approx \frac{d^2E^2}{2\hbar^2} \sum_{v' \leq v'_{\mathrm{max}}} \frac{\langle a|v'\rangle \langle v'|m\rangle}{\Delta_{v'}} - \frac{d^2E^2}{2\hbar^2\Delta_{\mathrm{thresh}}} \sum_{v' \leq v'_{\mathrm{max}}} \langle a|v'\rangle \langle v'|m\rangle . \tag{S.6}$$

We can account for the atomic continuum in the scattering rate in a similar way

$$\Gamma_{\mathrm{s}} \approx \frac{d^2E^2}{2\hbar^2} \sum_{v' \leq v'_{\mathrm{max}}} \Gamma_{v'} \frac{\langle m|v'\rangle \langle v'|m\rangle}{\Delta_{v'}^2} + \frac{d^2E^2\Gamma}{2\hbar^2\Delta_{\mathrm{thresh}}^2} \sum_{v' > v'_{\mathrm{max}}} \langle m|v'\rangle \langle v'|m\rangle , \tag{S.7}$$

where $\Gamma_{v'}$ is the excited state linewidth for the $|v'\rangle$ state, and we have assumed the atomic continuum states all have the same linewidth Γ. Using normalization, we derive an expression for the sum in the second term

$$\sum_{v' > v'_{\mathrm{max}}} \langle m|v'\rangle \langle v'|m\rangle = 1 - \sum_{v' \leq v'_{\mathrm{max}}} \langle m|v'\rangle \langle v'|m\rangle . \tag{S.8}$$

We then arrive at an expression for the scattering rate, accounting for the atomic continuum,

$$\Gamma_{\mathrm{s}} \approx \frac{d^2E^2}{2\hbar^2} \sum_{v' \leq v'_{\mathrm{max}}} \Gamma_{v'} \frac{\langle m|v'\rangle \langle v'|m\rangle}{\Delta_{v'}^2} + \frac{d^2E^2\Gamma}{2\hbar^2\Delta_{\mathrm{thresh}}^2} \left(1 - \sum_{v' \leq v'_{\mathrm{max}}} \langle m|v'\rangle \langle v'|m\rangle \right) . \tag{S.9}$$

We have replaced the full continuum with an effective state at the atomic threshold with strength proportional to the amount of wavefunction overlap between the target molecular state and all atomic continuum states. This model leads to a component in the scattering rate that is proportional to $1/\Delta_{\mathrm{thresh}}^2$ and is smaller as one detunes farther from the threshold. We note that the first term can also scale nearly as $1/\Delta_{\mathrm{thresh}}^2$, if, as in our case, the largest terms in the summation are from states near the threshold.

A very similar result holds for the light shift δ and is written here for completeness

$$\delta = \frac{d^2E^2}{2\hbar^2} \sum_{v' \leq v'_{\mathrm{max}}} \frac{\langle m|v'\rangle \langle v'|m\rangle}{\Delta_{v'}} + \frac{d^2E^2}{2\hbar^2\Delta_{\mathrm{thresh}}} \left(1 - \sum_{v' \leq v'_{\mathrm{max}}} \langle m|v'\rangle \langle v'|m\rangle \right) . \tag{S.10}$$

S3. COMPUTATIONAL METHODS FOR BOUND AND SCATTERING STATES

For scattering and near-threshold bound states, we solve the Schrödinger equation by coupled-channel methods [S1], using a basis set in which the electron spins $s_{\rm Na}$ and $s_{\rm Cs}$ and the nuclear spins $i_{\rm Na}$ and $i_{\rm Cs}$ are separately coupled,

$$|(s_{\rm Na}s_{\rm Cs}S)(i_{\rm Na}i_{\rm Cs}I)FM_F\rangle. \tag{S.11}$$

Here S and I are the total electron and nuclear spins of the molecule or atomic pair. Their resultant F is the total spin, with projection M_F onto the axis of the magnetic field. In principle F can be further coupled to the rotational angular momentum L, but in the present work only functions with $L = 0$ are included. In the absence of a magnetic field, F and M_F are both good quantum numbers, but in a magnetic field only M_F is conserved. The calculations in this paper use basis sets with all possible values of S, I and F (for the required value of M_F) that can be constructed with $s_{\rm Na} = s_{\rm Cs} = 1/2$, $i_{\rm Na} = 3/2$ and $i_{\rm Cs} = 7/2$.

Scattering calculations are carried out using the MOLSCAT package [S2, S3] and bound-state calculations using the related BOUND package [S3, S4]. The calculations use singlet and triplet interaction potentials for Na+Cs obtained by adjusting the potentials of Docenko *et al.* [S5] at short range, using the same procedure as for KCs [S6], to reproduce the experimental binding energy of the least-bound triplet state [S7] and the position of the s-wave Feshbach resonance near 864 G [S8]. The atomic nuclear hyperfine coupling and Zeeman effects are fully included, using the Hamiltonian described in [S9].

The bound-state calculations were initially used to predict the binding energies of states that lie within about 1 GHz of each atomic threshold of interest. At zero magnetic field, the states fall into groups from each hyperfine state of the atomic pair, labeled by $(f_{\rm Na}, f_{\rm Cs})$. For example, for the $(f_{\rm Na}, f_{\rm Cs}) = (2, 3)$ states that are of principal interest here, each group comprises 5 zero-field levels with $F = 1, 2, 3, 4$ and 5; one such group is spread out over a range of energies between 290 MHz and 770 MHz below the $(f_{\rm Na}, f_{\rm Cs}) = (2, 3)$ threshold. In a magnetic field, each zero-field level splits into $2F + 1$ Zeeman sublevels labeled by M_F. For each sublevel we can calculate the dependence of the energy on magnetic field, in order to choose a target state for which the Raman transition frequency depends only weakly on field.

The state that we ultimately chose as the target state for Raman transfer is the least-bound $(F, M_F) = (5, 5)$ sublevel with $(f_{\rm Na}, f_{\rm Cs}) = (2, 3)$, which was predicted at a binding energy 763 MHz below the $(f_{\rm Na}, f_{\rm Cs}) = (2, 3)$ threshold. As described in the text, it was subsequently located experimentally at a binding energy of 770.1969(2)MHz at 8.83(2)G.

Multichannel bound-state wavefunctions, with components labeled by S, I and F, are calculated using the method of Thornley and Hutson [S10]. For molecular bound states, they are obtained on a grid of internuclear distances from 2.4 Å to 50 Å. For states of confined atomic pairs, a harmonic confining potential is added to the molecular potentials and the grid is extended to 3000 Å.

S4. EXCITED MOLECULAR STATES

To obtain a full calculation for the expected Raman Rabi frequency, light shift and scattering, we need to account for all the excited molecular states. The lowest eight excited molecular potentials in NaCs asymptote to the dissociation limit of Na 3S + Cs 6P. These eight potentials can be written in the Hund's case (a) basis as $c^3\Sigma^+_{\Omega=0^-}, c^3\Sigma^+_{\Omega=1}, b^3\Pi_{\Omega=0^-}, b^3\Pi_{\Omega=0^+}, b^3\Pi_{\Omega=1}, b^3\Pi_{\Omega=2}, B^1\Pi_{\Omega=1}, A^1\Sigma^+_{\Omega=0^+}$ [S11]. Due to spin-orbit coupling, especially large in Cs, the excited molecular states are mixed, containing components in multiple potentials. Fortunately, single-channel potential energy curves for $c^3\Sigma^+_1$ and $B^1\Pi_1$ have been experimentally determined, and are predictive across the entire energy range of the potential [S12–S14]. Since there is only one $\Omega = 2$ potential at this dissociation limit, a single-channel potential has been determined for $b^3\Pi_2$ as well [S15]. Unfortunately, single-channel potentials for the other electronic states do not exist. A deperturbation analysis was required for states belonging to the mixed $A - b$ complex, and the fitted potentials and spin-orbit coupling coefficients are only accurate within the energy range of the measured experimental data [S16]. Since our experiment attempts to work in a regime where the predominant Raman coupling comes from the $v' = 0$ state of $c^3\Sigma^+_1$, the contribution of the other seven potentials is mainly to a background that is nearly detuning independent. Thus, for computational ease, we use the diabatic potentials for $b^3\Pi_0, b^3\Pi_1$ and $A^1\Sigma^+_{0^+}$. Lastly, to our knowledge, no potential fit to experimental data exists for the $c^3\Sigma^+_{0^-}$ state. Assuming that its contribution is only to the background, as an approximation, we simply double the contribution of all states except $v' = 0$ from $c^3\Sigma^+_1$.

S5. CALCULATING MATRIX ELEMENTS WITH COUPLED CHANNEL GROUND STATE

To calculate Rabi frequencies for transitions to the eight excited molecular potentials, we obtain their wavefunctions from a single-channel calculation [S17] using the potential energy curves described in section S4. We then calculate overlap integrals between these functions and either the triplet ($S = 1$) or singlet ($S = 0$) components of the coupled-channel wavefunctions for either the target molecular state or the confined atomic state. These calculations assume that the intermediate states have pure singlet or triplet character and neglect its nuclear spin character, which is unknown. These calculations include theoretical electronic transition dipole moments shown in figure S1 calculated with *ab initio* methods [S18].

The full calculation of the Raman Rabi frequency and scattering rate using the methods in section S2 is shown in figure S2. The strong contribution from the atomic threshold arises from the large overlap to the near-threshold bound states shown in figure S3 for the $c^3\Sigma_1^+$ state. This leads to a $1/\Delta^2_{\mathrm{thresh}}$ dependence of the scattering rate and favors using deeply bound states as the intermediate state for the Raman transfer. A similar result holds for the other excited state potentials.

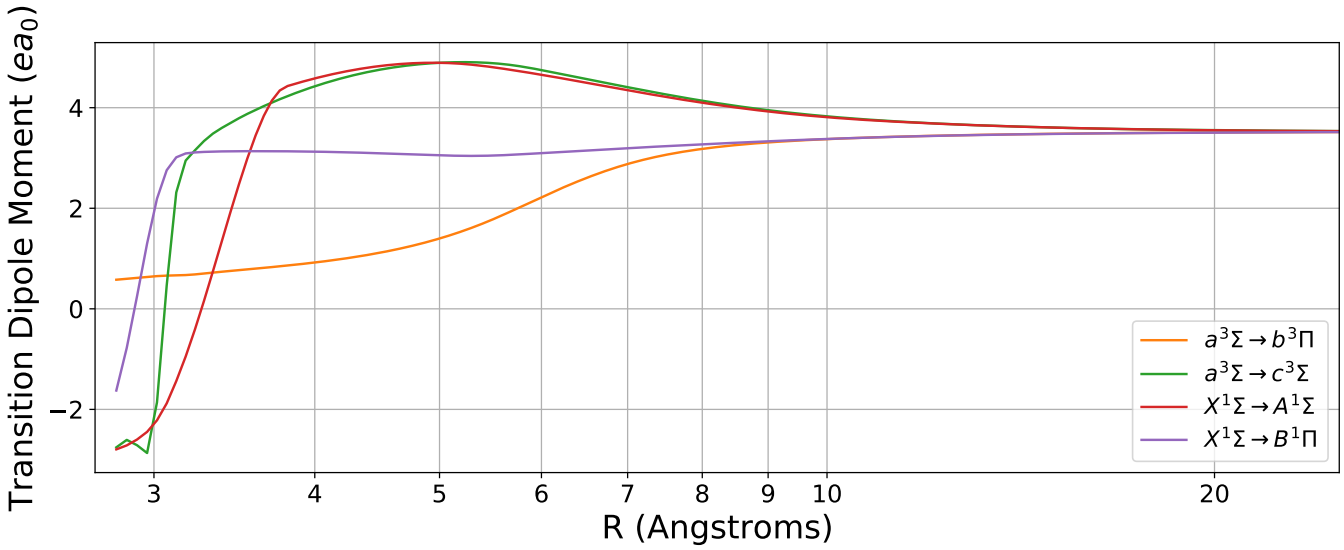

FIG. S1. Electronic transition dipole moments calculated via *ab initio* methods between different electronic states of NaCs. These transition dipole moments are shown in units of ea_0, where e is the elementary charge and a_0 is the Bohr radius. They are plotted as a function of internuclear distance, R.

S6. EFFECTIVE MATRIX ELEMENTS TO A SINGLE STATE

In this calculation, there is a matrix element, $\Omega_{\mathrm{a}ij}, \Omega_{\mathrm{m}ij}$ between each channel i of the coupled channel ground state and an excited state j. The total Raman Rabi frequency Ω_{R}, light shift δ and off-resonant scattering Γ_{s} contribution from this single excited state is calculated as

$$\Omega_{\mathrm{R}j} = \sum_i \frac{\Omega_{\mathrm{a}ij}\Omega_{\mathrm{m}ij}}{2\Delta}, \tag{S.12}$$

$$\delta_j = \sum_i \frac{\Omega^2_{\mathrm{a}ij} - \Omega^2_{\mathrm{m}ij}}{2\Delta}, \tag{S.13}$$

$$\Gamma_{\mathrm{s}j} = \sum_i \Gamma_{\mathrm{e}} \frac{\Omega^2_{\mathrm{a}ij} + \Omega^2_{\mathrm{m}ij}}{2\Delta^2}, \tag{S.14}$$

where Δ is the single photon detuning and Γ_{e} is the excited state linewidth. The experiment, through measuring the detuning dependence of the Raman Rabi frequency and the resonance frequency, extracts a single Ω_{m} and Ω_{a}. In

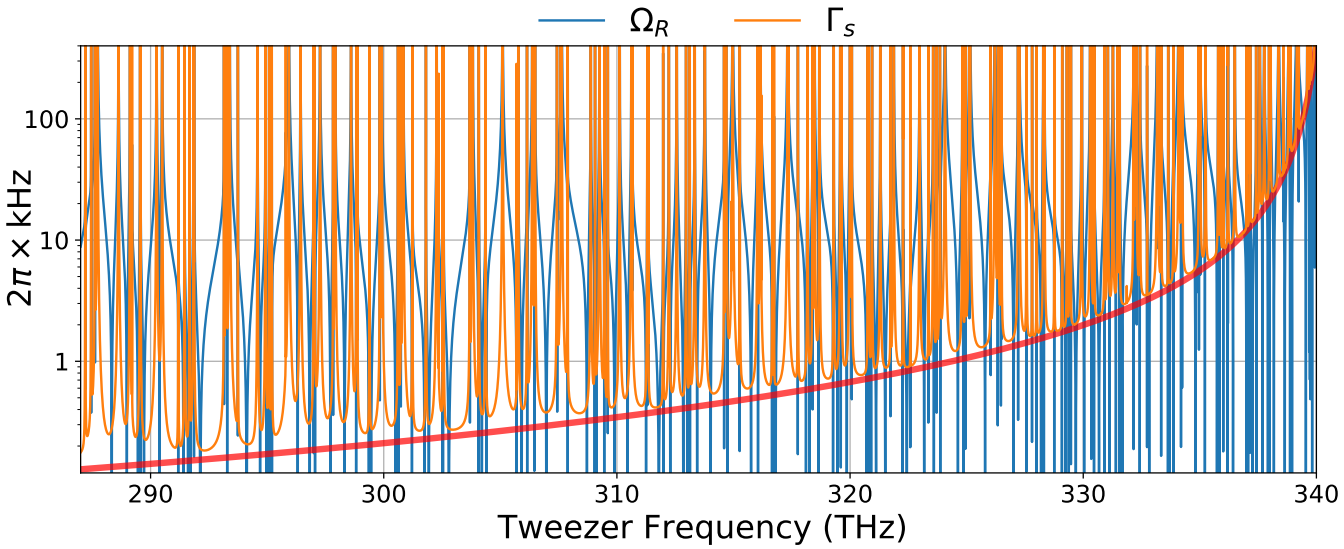

FIG. S2. Full calculation of the Raman Rabi frequency and scattering rate as a function of the single-photon frequency including all vibrational states of $c^3\Sigma^+(\Omega = 1)$ and the atomic continuum. The second frequency in the Raman transition is offset by about 770 MHz and resonant with the two photon transition. The assumed excited-state linewidth for all molecular lines is 50 MHz. The red line shows the contribution that comes only from the near-threshold states.

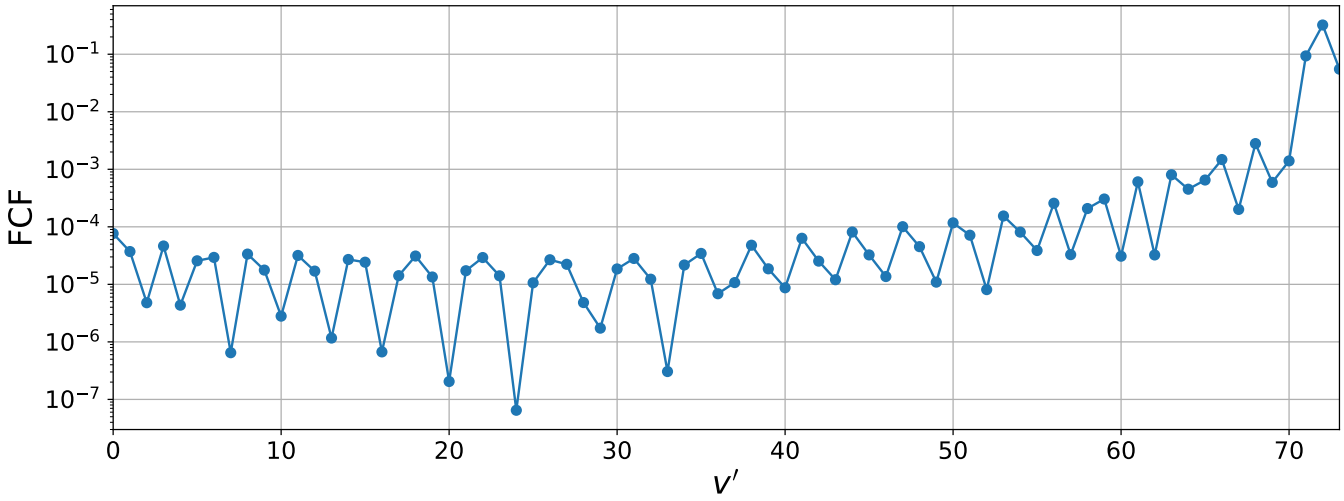

FIG. S3. The Franck-Condon Factor (FCF) between the target molecular state and vibrational state v' of $c^3\Sigma_1^+$. The potential supports 74 bound states, and the predominant contribution arises from the near-threshold bound states. The total overlap with all the bound states is 0.4822, which is 96.8% of the total triplet fraction of the target molecular state.

order to compare to the theory, we introduce effective $\Omega'_{\rm a}, \Omega'_{\rm m}, \Gamma'_{\rm e}$, so that $\Omega_{\rm R} = \Omega'_{\rm a}\Omega'_{\rm m}/(2\Delta)$, $\delta = (\Omega'^2_{\rm a} - \Omega'^2_{\rm m})/(2\Delta)$, and $\Gamma_{\rm s} = \Gamma'_{\rm e}(\Omega'^2_{\rm a} + \Omega'^2_{\rm m})/(2\Delta^2)$. The effective Rabi frequencies for the $v' = 0$ state of $c^3\Sigma_1^+$ and their ratio are reported in Table S1 at 3.75 mW of tweezer power.

S7. SCALING OF ATOMIC MATRIX ELEMENT WITH TWEEZER POWER

Since our coupled-channel calculations include the harmonic confinement, we can calculate the enhancement in $\Omega_{\rm a}$ with increasing confinement. Using two calculations with $\omega_{\rm trap} = 36.5$ kHz and $\omega_{\rm trap} = 80$ kHz trapping frequencies, and assuming a power law scaling, we find that the wavefunction overlap scales as $\omega_{\rm trap}^{0.58} = P^{0.29}$. Thus, $\Omega_{\rm a} \propto P^{0.79}$, which was also experimentally verified. However, we note that in the actual experiment, our system does not have

$\Omega'_{\rm m}$	$2\pi \times 573$ MHz
$\Omega'_{\rm a}$	$2\pi \times 7.37$ MHz
$\Omega'_{\rm a}/\Omega'_{\rm m}$	0.013

TABLE S1. The effective Rabi frequencies for the $v' = 0$ state of $c^3\Sigma_1^+$ at 3.75 mW of tweezer power.

spherically symmetric confinement. The radial trapping frequency is about 5.7 times larger than the axial trapping frequency.

[S1] J. M. Hutson, Coupled channel methods for solving the bound-state schrödinger equation, Comp. Phys. Commun. **84**, 1 (1994).

[S2] J. M. Hutson and C. R. Le Sueur, MOLSCAT: a program for non-reactive quantum scattering calculations on atomic and molecular collisions, Comp. Phys. Commun. **241**, 9 (2019).

[S3] J. M. Hutson and C. R. Le Sueur, MOLSCAT, BOUND and FIELD, version 2020.0, https://github.com/molscat/molscat (2020).

[S4] J. M. Hutson and C. R. Le Sueur, BOUND and FIELD: programs for calculating bound states of interacting pairs of atoms and molecules, Comp. Phys. Commun. **241**, 1 (2019).

[S5] O. Docenko, M. Tamanis, J. Zaharova, R. Ferber, A. Pashov, H. Knöckel, and E. Tiemann, The coupling of the $x^1\sigma^+$ and $x^3\sigma^+$ states of the atom pair na + cs and modelling cold collisions, J. Phys. B **39**, S929 (2006).

[S6] M. Gröbner, P. Weinmann, E. Kirilov, H.-C. Nägerl, P. S. Julienne, C. R. Le Sueur, and J. M. Hutson, Observation of interspecies feshbach resonances in an ultracold ^{39}K $-^{133}$ Cs mixture and refinement of interaction potentials, Phys. Rev. A **95**, 022715 (2017).

[S7] J. D. Hood, Y. Yu, Y.-W. Lin, J. T. Zhang, K. Wang, L. R. Liu, B. Gao, and K.-K. Ni, Multichannel interactions of two atoms in an optical tweezer, Phys. Rev. Research **2**, 023108 (2020).

[S8] J. T. Zhang, Y. Yu, W. B. Cairncross, K. Wang, L. R. B. Picard, J. D. Hood, Y.-W. Lin, J. M. Hutson, and K.-K. Ni, Forming a single molecule by magnetoassociation in an optical tweezer, Phys. Rev. Lett. **124**, 253401 (2020).

[S9] J. M. Hutson, E. Tiesinga, and P. S. Julienne, Avoided crossings between bound states of ultracold cesium dimers, Phys. Rev. A **78**, 052703 (2008).

[S10] A. E. Thornley and J. M. Hutson, Bound-state wave functions from coupled channel calculations using log-derivative propagators: Application to spectroscopic intensities in ar-hf, J. Chem. Phys. **101**, 5578 (1994), https://doi.org/10.1063/1.467345.

[S11] M. Korek, S. Bleik, and A. R. Allouche, Theoretical calculation of the low laying electronic states of the molecule nacs with spin-orbit effect, J. Chem. Phys. **126**, 124313 (2007).

[S12] A. Grochola, P. Kowalczyk, and W. Jastrzebski, Investigation of the $B^1\Pi$ state in NaCs by polarisation labelling spectroscopy, Chemical Physics Letters **497**, 22 (2010).

[S13] A. Grochola, P. Kowalczyk, J. Szczepkowski, W. Jastrzebski, A. Wakim, P. Zabawa, and N. P. Bigelow, Spin-forbidden $c^3\Sigma^+(\Omega = 1) \leftarrow X^1\Sigma^+$ transition in nacs: Investigation of the $\Omega = 1$ state in hot and cold environments, Phys. Rev. A **84**, 012507 (2011).

[S14] L. R. Liu, J. T. Zhang, Y. Yu, N. R. Hutzler, Y. Liu, T. Rosenband, and K.-K. Ni, Ultracold Molecular Assembly, arXiv:1701.03121 (2017).

[S15] P. J. Zabawa, *Production of Ultracold, Absolute Vibrational Ground State NaCs Molecules*, Ph.D. thesis, University of Rochester (2012).

[S16] J. Zaharova, M. Tamanis, R. Ferber, A. N. Drozdova, E. A. Pazyuk, and A. V. Stolyarov, Solution of the fully-mixed-state problem: Direct deperturbation analysis of the $A^1\Sigma^+ - b^3\Pi$ complex in a nacs dimer, Phys. Rev. A **79**, 012508 (2009).

[S17] E. Fattal, R. Baer, and R. Kosloff, Phase space approach for optimizing grid representations: The mapped fourier method, Phys. Rev. E **53**, 1217 (1996).

[S18] Private communication with R. Moszynski.